博 士 学 位 論 文

バーチャルスライド WSI を用いた

卵巣高異型度漿液性癌の病理形態学的細分類

近 畿 大 学 大 学 院

医 学 研 究 科 医 学 系 専 攻

宮 川 知 保

Doctoral Dissertation

Histopathological subtyping

of high-grade serous ovarian cancer

using whole slide imaging

November 2023

Major in Medical Sciences
Kindai University Graduate School of Medical Sciences

Chiho Miyagawa

同 意 書

2023 年 11 月 2 日

近畿大学大学院
医学研究科長　殿

共著者　中井英勝　㊞　　共著者　高村史記　㊞

共著者　髙文子玄　㊞　　共著者　＿＿＿＿＿＿＿　㊞

共著者　松村謙臣　㊞　　共著者　＿＿＿＿＿＿＿　㊞

共著者　大谷知之　㊞　　共著者　＿＿＿＿＿＿＿　㊞

論文題目

Histopathological subtyping of high-grade serous ovarian cancer
using whole slide imaging

下記の博士論文提出者が、標記論文を貴学医学博士の学位論文（主論文）

として使用することに同意いたします。

また、標記論文を再び学位論文として使用しないことを誓約いたします。

記

1．博士論文提出者氏名　　　　　　　　　　宮川　知保

2．専攻分野　　医学系　　　　　　　　　　女性機能病態・周産期医学

<div align="center">

同　意　書

</div>

2023 年 11 月 2 日

近畿大学大学院
　医学研究科長　殿

共著者　万代昌紀 ㊞　　　　　共著者　＿＿＿＿＿＿＿ ㊞

共著者　村上隆介 ㊞　　　　　共著者　＿＿＿＿＿＿＿ ㊞

共著者　＿＿＿＿＿＿＿ ㊞　　共著者　＿＿＿＿＿＿＿ ㊞

共著者　＿＿＿＿＿＿＿ ㊞　　共著者　＿＿＿＿＿＿＿ ㊞

論文題目

　Histopathological subtyping of high-grade serous ovarian cancer
　using whole slide imaging

下記の博士論文提出者が、標記論文を貴学医学博士の学位論文（主論文）

として使用することに同意いたします。

また、標記論文を再び学位論文として使用しないことを誓約いたします。

<div align="center">

記

</div>

１．博士論文提出者氏名　　　　　　　　　　宮川　知保

２．専攻分野　　医学系　　　　　　　　　　女性機能病態・周産期医学

<div align="right">

近畿大学大学院医学研究科

</div>

同　意　書

2023年 10月 2 日

近畿大学大学院
　医学研究科長　殿

共著者　村上幸祐　㊞　　　　　　共著者　＿＿＿＿＿＿＿＿＿　㊞

共著者　＿＿＿＿＿＿＿＿＿　㊞　　　　　　共著者　＿＿＿＿＿＿＿＿＿　㊞

共著者　＿＿＿＿＿＿＿＿＿　㊞　　　　　　共著者　＿＿＿＿＿＿＿＿＿　㊞

共著者　＿＿＿＿＿＿＿＿＿　㊞　　　　　　共著者　＿＿＿＿＿＿＿＿＿　㊞

論文題目

Histopathological subtyping of high-grade serous ovarian cancer
using whole slide imaging

下記の博士論文提出者が、標記論文を貴学医学博士の学位論文（主論文）

として使用することに同意いたします。

また、標記論文を再び学位論文として使用しないことを誓約いたします。

記

1．博士論文提出者氏名　　　　　　　　　　宮川　知保

2．専攻分野　　医学系　　　　　　　　女性機能病態・周産期医学

近畿大学大学院医学研究科

JOURNAL OF
GYNECOLOGIC
ONCOLOGY

Original Article

Check for updates

Histopathological subtyping of high-grade serous ovarian cancer using whole slide imaging

Chiho Miyagawa [iD],[1] Hidekatsu Nakai [iD],[1] Tomoyuki Otani [iD],[2]
Ryusuke Murakami [iD],[3] Shiki Takamura [iD],[4] Hisamitsu Takaya [iD],[1]
Kosuke Murakami [iD],[1] Masaki Mandai [iD],[3] Noriomi Matsumura [iD] [1]

[1]Department of Obstetrics and Gynecology, Kindai University Faculty of Medicine, Osaka-Sayama, Japan
[2]Department of Pathology, Kindai University Faculty of Medicine, Osaka-Sayama, Japan
[3]Department of Gynecology and Obstetrics, Graduate School of Medicine, Kyoto University, Kyoto, Japan
[4]Department of Immunology, Kindai University Faculty of Medicine, Osaka-Sayama, Japan

OPEN ACCESS

Correspondence to
Hidekatsu Nakai
Department of Obstetrics and Gynecology, Kindai University Faculty of Medicine, 377-2 Ohno-higashi, Osaka-Sayama, Osaka 589-8511, Japan.
Email: nakai@med.kindai.ac.jp

ORCID iDs
Chiho Miyagawa [iD]
https://orcid.org/0000-0002-9614-0117
Hidekatsu Nakai [iD]
https://orcid.org/0000-0002-9994-2131
Tomoyuki Otani [iD]
https://orcid.org/0000-0002-4351-324X
Ryusuke Murakami [iD]
https://orcid.org/0000-0001-5007-5674
Shiki Takamura [iD]
https://orcid.org/0000-0001-6681-0258
Hisamitsu Takaya [iD]
https://orcid.org/0000-0002-5234-9226

ABSTRACT

Objective: We have established 4 histopathologic subtyping of high-grade serous ovarian cancer (HGSOC) and reported that the mesenchymal transition (MT) type has a worse prognosis than the other subtypes. In this study, we modified the histopathologic subtyping algorithm to achieve high interobserver agreement in whole slide imaging (WSI) and to characterize the tumor biology of MT type for treatment individualization.

Methods: Four observers performed histopathological subtyping using WSI of HGSOC in The Cancer Genome Atlas data. As a validation set, cases from Kindai and Kyoto Universities were independently evaluated by the 4 observers to determine concordance rates. In addition, genes highly expressed in MT type were examined by gene ontology term analysis. Immunohistochemistry was also performed to validate the pathway analysis.

Results: After algorithm modification, the kappa coefficient, which indicates interobserver agreement, was greater than 0.5 (moderate agreement) for the 4 classifications and greater than 0.7 (substantial agreement) for the 2 classifications (MT vs. non-MT). Gene expression analysis showed that gene ontology terms related to angiogenesis and immune response were enriched in the genes highly expressed in the MT type. CD31 positive microvessel density was higher in the MT type compared to the non-MT type, and tumor groups with high infiltration of CD8/CD103 positive immune cells were observed in the MT type.

Conclusion: We developed an algorithm for reproducible histopathologic subtyping classification of HGSOC using WSI. The results of this study may be useful for treatment individualization of HGSOC, including angiogenesis inhibitors and immunotherapy.

Keywords: Carcinoma; Ovarian Epithelial Cancer; Biomarkers; Histopathology

Synopsis

We developed an algorithm for the histopathological subtyping of high-grade serous ovarian cancer (HGSOC) using whole slide imaging. We found that this classification may be associated with response to bevacizumab and immune-checkpoint inhibitors. This study would be useful for individualizing the treatment of HGSOC.

Generated by xmlinkpress

Kosuke Murakami
https://orcid.org/0000-0003-4278-5849
Masaki Mandai
https://orcid.org/0000-0003-4428-8029
Noriomi Matsumura
https://orcid.org/0000-0002-4512-7975

Conflict of Interest

No potential conflict of interest relevant to this article was reported.

Author Contributions

Conceptualization: M.C., M.R., M.M., M.N., N.H.; Data curation: M.C., O.T., M.R., T.S., N.H.; Formal analysis: M.C., M.R., T.H., M.K., M.N.; Funding acquisition: M.N., N.H.; Methodology: M.C., O.T., M.R., M.N., N.H.; Software: T.H., M.N.; Supervision: M.M., M.N.; Writing - original draft: M.C., M.N.; Writing - review & editing: M.C., O.T., M.R., T.S., T.H., M.K., M.M., M.N., N.H.

INTRODUCTION

Ovarian cancer has the poorest prognosis among all gynecologic malignancies with an overall 5-years survival rate of approximately 50% [1]. High-grade serous ovarian cancer (HGSOC) is the most common histopathological type of ovarian cancer [2]. Hallmarks of HGSOC are mainly *BRCA1/2* mutations and homologous recombination deficiency (HRD) and maintenance treatment with poly ADP-ribose polymerase (PARP) inhibitor is also used, after first-line chemotherapy [3]. Besides, maintenance therapy with bevacizumab, an anti-vascular endothelial growth factor (VEGF) antibody, is another option. However, several phase III trials showed that bevacizumab only extends the median progression-free survival (PFS) by 3.8 months [4] or 1.5 months [5]. Another option in chemotherapy regimens for ovarian cancer is dose-dense (dd) paclitaxel and carboplatin (TC), which increases the dose of paclitaxel. The Japanese Gynecologic Oncology Group (JGOG) 3016 study showed that ddTC therapy prolonged PFS and overall survival compared with TC therapy [6,7]. However, subsequent clinical trials did not prove the benefit of ddTC [8].

The Cancer Genome Atlas (TCGA) data analysis revealed that HGSOC can be classified into 4 gene expression subtypes [9]: mesenchymal, proliferative, immunoreactive, and differentiated, and the efficacy of bevacizumab was reported to be higher in the first 2 [10]. On the other hand, we previously showed that the mesenchymal type is more sensitive to taxane and ddTC may be useful for patients with this subtype [11]. Thus, gene expression analysis may be useful to select patients who would benefit from bevacizumab or ddTC. However, this is difficult to implement in daily practice because of problems with cost and sample quality assurance. Therefore, we used conventional hematoxylin and eosin (HE) glass slides to histopathologically characterize 4 subtypes of HGSOC, mesenchymal transition (MT), solid and proliferative (SP), immune reactive (IR), and papilloglandular (PG) [12]. Among them, the association between histopathological MT and TCGA Mesenchymal types was strong. We then reviewed the HE slides of HGSOC cases enrolled in the JGOG3016 study and found that ddTC was useful in the MT type [13].

In the research to create a new algorithm for histopathological subtyping, the use of HE slides has limitations in terms of sample transportation, storage, and personal information protection, making it difficult to prove the reproducibility of diagnosis and achieve clinical application. Virtual slides (whole slide imaging, WSI), which are digitalized representative slides of the tumor, can be stored, and copied electronically, and it is easy to evaluate the inter-observer agreement. The WSI data of HGSOC in TCGA are publicly available and can be observed by pathologists around the world. In addition, many recent clinical trials have preserved WSI of representative tumor slides. Therefore, establishing an evaluation method using WSI will allow us to retrospectively investigate the relationship with clinical trial outcomes.

In this study, we demonstrate that histopathological subtyping of HGSOC can be performed using WSI. We also show the relationship between the MT subtype and tumor biology, which may lead to the selection of targeted therapies. These findings will contribute to the implementation of personalized therapy based on the histopathology of HGSOC.

MATERIALS AND METHODS

1. TCGA data analysis

WSI data for ovarian cancer were available for 106 cases in the Genomic Data Commons data portal (https://portal.gdc.cancer.gov/). The annotation of HRD scores and *BRCA1/2* alterations (germline and somatic *BRCA1/2* mutations and *BRCA1* promoter methylations) in TCGA database was based on our previous report [14].

Inter-observer agreement

Four observers (M.C., N.H., O.T., and M.R.) specializing in gynecologic pathology and oncology and including one board-certified pathologist (O.T.), evaluated the characteristics of WSI and classified them into MT, IR, PG, and SP histopathological types based on our previously established algorithm [12]. The newly constructed algorithm is detailed in **Fig. 1A, B** and **Data S1**. As an overview, first, MT is diagnosed when tumor cell clusters with labyrinthine architecture or cells lacking continuity that infiltrate with stromal reaction are present in more than 10% of the slide. In addition, IR is diagnosed when lymphocytes infiltrating the stroma are present in 25% or more of the slide (**Fig. S1**). If these are not met, determine the form with the largest occupied area (SP or PG). The discordant cases were discussed, and the diagnostic methods were clarified to increase the agreement rate. Two observers (M.C. and O.T.) assessed Solid, pseudo-Endometrioid, and Transitional cell carcinoma-like morphology (SET) features [15]. Interobserver agreement of the histopathological subtyping was evaluated with Cohen's (2 observers) or Fleiss' (4 observers) kappa coefficient using irr package in R (R Foundation, Vienna, Austria). Kappa of 0–0.2 is slight, 0.2–0.6 moderate, 0.6–0.8 substantial, 0.8–1 almost perfect agreement.

Gene expression analysis

For gene expression microarray analysis, TCGA HG-U133A data set was obtained from TCGA Data Portal (http://cancergenome.nih.gov). The Affymetrix array data were RMA normalized using the R package affy (http://www.R-project.org). Single-sample Gene Set Enrichment Analysis (ssGSEA) was performed as previously described [12]. For data analyses, the ssGSEA scores were normalized from 0 to 1. Genes highly expressed in the MT type were identified using samroc [16] with false discovery rates (FDR) q<0.05 as a cutoff. The Gene Ontology term (biological process) enriched in the genes was identified using GO net [17], and the network was visualized.

2. The Kindai/Kyoto cohort data analysis

Fifty-nine HGSOC cases that underwent surgery between 2007 and 2018 at Kindai University Hospital and Kyoto University Hospital were included in the study. Formalin-fixed paraffin-embedded samples of untreated tumors were retrieved, and HE slides of representative tumor sections were digitized. The WSI data were observed using the NanoZoomer Digital Pathology System view 2.8.24 (Hamamatsu Photonics K.K., Hamamatsu, Japan).

Inter-observer agreement

Four observers (M.C., N.H., O.T., and M.R.) independently assessed the WSI data, and the agreement rate of histopathological subtyping diagnosis was examined.

Immunohistopathological staining

Formalin-fixed paraffin-embedded sections were cut into sections (3 μm thick) and heated in DAKO Target Retrieval Solution (S1699; Dako, Santa Clara, CA, USA), diluted 1:10 in
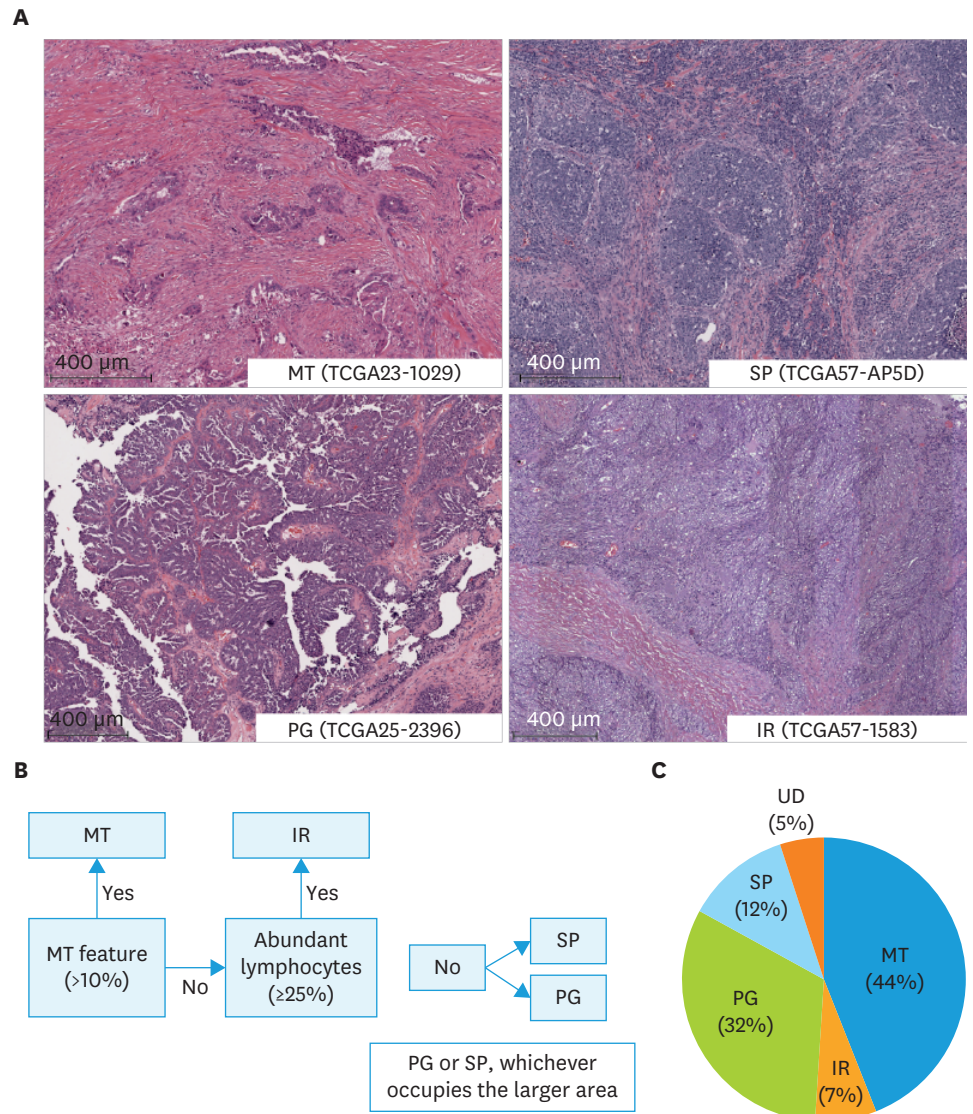
Fig. 1. Histopathological subtyping of high-grade serous ovarian cancer using The Cancer Genome Atlas whole slide imaging. (A) Representative images of histopathologic subtypes. MT: glandular ducts and cells infiltrating with stromal reaction occupy ≥10% of the specimen; IR: lymphocytes infiltrating in the stroma occupy ≥25%. (B) Hierarchy of subtyping. (C) Proportion of each subtype.
IR, immune reactive; MT, mesenchymal transition; PG, papillary proliferation; SP, solid proliferation; UD, undetermined.

distilled water pH 6, at 98°C for 50 minutes. Endogenous proteins were blocked with Animal-Free Blocker (SP5030, 1:4; Vector, New York, NY, USA), and samples were incubated for 15 minutes at room temperature (RT).

For immunohistochemical staining of CD31, CD8 and CD103 sections were incubated with CD31 antibody (C31.3, 1:100; Novus Biologicals, Centennial, CO, USA), CD8 antibody (LCL-L-CD8-4B11, 1:250; Leica Biosystems, Nussloch, Germany) and CD103 antibody (ab129202, 1:6,000; Abcam, Cambridge, UK) at 4°C overnight. Sections were washed, and 3% H_2O_2/PBS was applied for 15 minutes to block peroxidase. DAB (3:100; Vector), Fast Red (415261; Nichirei Biosciences, Tokyo, Japan) and Histgreen (E109; LINARIS Biologische Produkt, Dossenheim, Germany) were added for 3 minutes at RT.

All immunohistochemically stained slides were digitized and quantitatively evaluated using QuPath v0.2.0 (https://qupath.github.io/) (**Data S2**). Microvessel density (MVD) was determined by counting the number of CD31-positive luminal structures per mm^2 at 5 representative tumor sites and calculating the mean value, as described in a previous report [18]. To quantify CD8$^+$ and/or CD103$^+$ staining, the number of positive cells per 1 mm^2 was counted for each sample using Qupath, and the mean value of 5 fields of view was calculated. The obtained values were used to perform average linkage clustering using Cluster 3.0, followed by visualization using Java TreeView 1.2.0.

3. Ethics approval
This study was approved by the ethics committees of Kindai University Hospital (the approval number; 31-146). All methods were performed in accordance with the ethical standards of the responsible committee on human experimentation (institutional and national) and with the Helsinki Declaration of 1964 and its later amendments. Informed consent was obtained in the form of an opt-out option on the website of the institution in 2020.

4. Statistical analysis
Statistical analysis was performed using GraphPad Prism ver. 8.2.0 (GraphPad Software, San Diego, CA, USA). Comparison among 3 or more groups was conducted with ordinary one-way analysis of variance and comparison between 2 groups was performed with t-test. $p < 0.05$ indicated a significant difference.

RESULTS

1. Histopathological subtyping of HGSOC using WSI
Histopathological subtyping of TCGA samples
Among the 106 TCGA ovarian cancer cases, 4 cases without *TP53* mutation [19] could not be diagnosed as HGSOC by pathomorphology and were excluded. We examined the WSI of the other 102 cases. First, based on the original definitions (**Fig. 1**) [12] and diagnosed independently by the 4 observers without training, the Fleiss' kappa coefficient was low with 4 subtypes, 0.348 (fair agreement), and binary classifications of MT vs. non-MT, 0.350 (fair agreement) (**Table S1**).

To improve the reproducibility of the diagnosis, the algorithm was clarified (**Data S1**). The summary is as follows: for MT, morphological characteristics of labyrinthine infiltrating cells with marked stromal reaction (i.e., micropapillary pattern, irregular glands, small nests, single cells) were specified. In addition, it was difficult to observe intraepithelial tumor infiltrating lymphocytes (TILs) in WSI. Therefore, based on the evaluation method of the TILs Working Group in Breast Cancer [20,21], only stromal TILs were counted, not intraepithelial TILs or TILs in necrotic tissue, with a cut-off of 25%. Regarding PG, we included not only the classical papillary form, but also low-grade endometrioid carcinoma like and serous borderline tumor like forms.

Next, the WSI data were independently re-evaluated by the 4 observers. The Fleiss' kappa coefficient increased to 0.549 (moderate agreement) for the 4 subtypes and 0.705 (substantial agreement) for the binary classifications (**Table 1**). Under the new algorithm, perfect agreement (4 out of 4 observers) for 4 and binary classifications was 48 cases (47%) and 56 cases (55%), majority agreement (3 out of 4 observers) was 77 cases (75%) and

Table 1. Inter-observer concordance rates for TCGA samples

Observers	Four classifications; Fleiss' kappa 0.549			Two classifications (MT vs. non-MT); Fleiss' kappa 0.705		
	N.H.	O.T.	M.R.	N.H.	O.T.	M.R.
M.C.	70% (0.56)	87% (0.81)	62% (0.48)	82% (0.65)	92% (0.84)	78% (0.58)
N.H.		67% (0.51)	63% (0.51)		83% (0.68)	80% (0.63)
O.T.			60% (0.46)			77% (0.57)

The numbers in parentheses represent Cohen's kappa coefficient.
TCGA, The Cancer Genome Atlas.

Table 2. Inter-observer concordance rates for the Kindai/Kyoto cohortThe numbers in parentheses represent Cohen's kappa coefficient.

Observers	Four classifications; Fleiss' kappa 0.588			Two classifications (MT vs. non-MT); Fleiss' kappa 0.703		
	N.H.	O.T.	M.R.	N.H.	O.T.	M.R.
M.C.	83% (0.76)	88% (0.83)	62% (0.49)	93% (0.86)	94% (0.90)	81% (0.59)
N.H.		67% (0.66)	58% (0.42)		92% (0.83)	78% (0.53)
O.T.			54% (0.39)			75% (0.50)

MT, mesenchymal transition.

86 cases (84%). Final histopathologic subtyping classification was agreed upon through observer discussion for 97 of the 102 cases and was used for subsequent analysis. MT, IR, PG, and SP accounted for 44%, 7%, 32%, and 12%, respectively (**Fig. 1C**). The remaining 5 cases could not be classified (Undetermined; UD). Two were cases with histomorphology that could not be classified even with the new classification algorithm; the presence of such cases is acknowledged at the bottom of the subtyping algorithm (**Data S1**). Three cases were not suitable for histological analysis because 2 had mostly stromal tissue with little or no neoplastic epithelium in the WSI available on the TCGA website and one had only frozen sections (**Fig. S2**).

Inter-observer agreement of the Kindai/Kyoto cohort
For assessment of inter-observer agreement and for later analysis of immunohistochemistry, 4 observers independently performed histopathological subtyping of WSI in the Kindai/Kyoto cohort (n=59). The Fleiss' kappa coefficient was 0.558 (moderate agreement) for the 4 classifications and improved to 0.703 (substantial agreement) for the binary classifications (MT and non-MT) (**Table 2**). Perfect agreement (4 out of 4 observers) for 4 and binary classifications was 23 cases (39%) and 39 cases (69%), majority agreement (3 out of 4 observers) was 46 cases (78%) and 54 cases (92%).

2. Molecular characteristics of HGSOC subtype
Relationship between HRD status and histopathological features
We found no association between the 4 subtypes and HRD scores or *BRCA* alterations (germline/somatic *BRCA1/2* mutations and *BRCA1* promoter methylations) (**Fig. S3**). Then SET features, previously reported to be associated with *BRCA* mutations [15], were evaluated in the 102 TCGA cases by 2 observers using WSI The concordance rate for SET cases (SET features ≥50%) was 79% (Cohen's kappa coefficient: 0.44) (**Table S2**). We compared these matched cases with our HGSOC histopathological subtyping, and the SP type was mostly SET cases (p<0.001, **Fig. S3**) because the histological images of "solid tumor" overlapped with those defined by SET. There was no association between SET features and *BRCA* alterations or HRD scores (**Fig. S3**).

Characterization of MT type by gene expression profiling
The MT type, which shows the poorest prognosis among the 4 subtypes [12], was investigated for its biological properties, with the aim to explore personalized therapy for MT. Of the 94 cases for which histopathological subtyping was performed, 84 cases had gene expression data
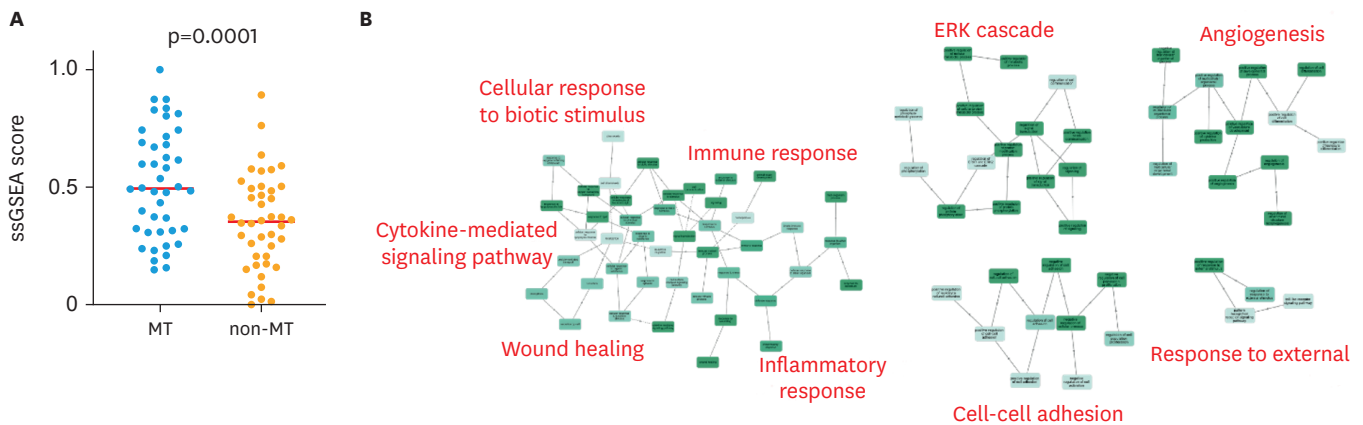
Fig. 2. Characteristics of MT type in gene expression profiles. (A) ssGSEA scores of an epithelial-mesenchymal transition-related gene set (HALLMARK_EPITHELIAL_MESENCHYMAL_TRANSITION). Y axis: normalized value of ssGSEA score. (B) Network diagram of gene ontology terms enriched in genes highly expressed in the MT type in The Cancer Genome Atlas dataset. Representative gene ontology terms are shown in red.
MT, mesenchymal transition; ssGSEA, single-sample Gene Set Enrichment Analysis.

available. We examined the ssGSEA scores of HALLMARK_EPITHELIAL_MESENCHYMAL_TRANSITION, genes defining epithelial-mesenchymal transition [22], on these data. The results showed that the MT type had a higher score than the other subtypes (p=0.001) (**Fig. 2**).

Additionally, we examined differentially expressed genes between MT and non-MT types. A total of 286 genes (380 probes) were highly expressed (FDR q < 0.05) in the MT type (**Table S3**). The gene ontology terms enriched in these genes (**Table S4**) were related to immune response, wound healing, ERK cascade, angiogenesis, and cell adhesion (**Fig. 2**).

Analysis of the angiogenesis pathway
Next, we searched for molecular targets in MT type. As bevacizumab is a clinically used anti-angiogenic drug for ovarian cancer, we focused on the angiogenesis pathway. The *PECAM1* gene (208983_s_at), which encodes CD31, a marker of vascular endothelium, was significantly upregulated in the MT type (p=0.007, **Fig. 3**). We next assessed CD31-positive MVD in 46 patients in the Kindai/Kyoto cohort (**Tables S5** and **S6**) in whom at least 3 out of 4 diagnoses were concordant. We found that MVD was significantly higher in the MT group than in the non-MT group (IR+PG+SP) (p=0.020, **Fig. 3**).
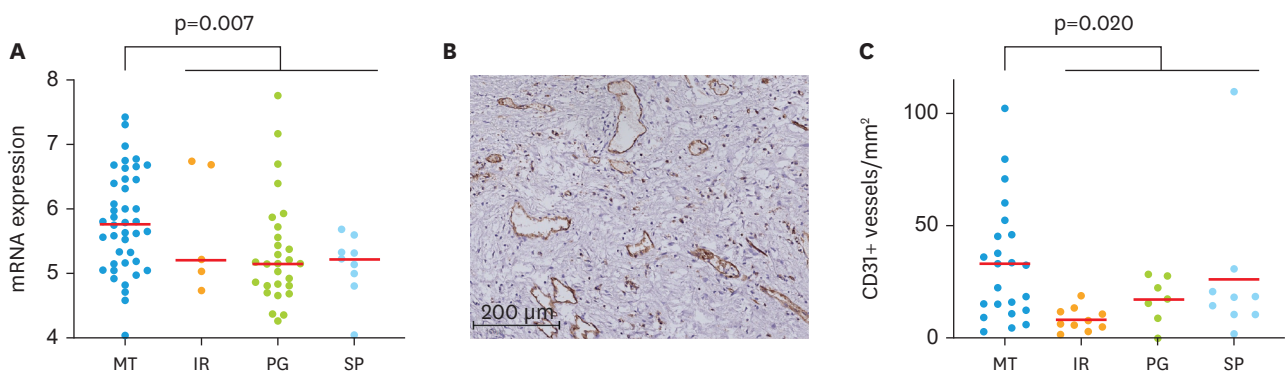

Fig. 3. Association of histopathologic subtypes of high-grade serous ovarian cancer with MVD. (A) Expression of *PECAM1* gene (208983_s_at) in The Cancer Genome Atlas dataset. (B) Representative image of CD31 immunohistochemistry. (C) Comparison of CD31+ MVD among histopathological subtypes.
IR, immune reactive; MT, mesenchymal transition; MVD, microvascular density; PG, papilloglandular; SP, solid and proliferative.
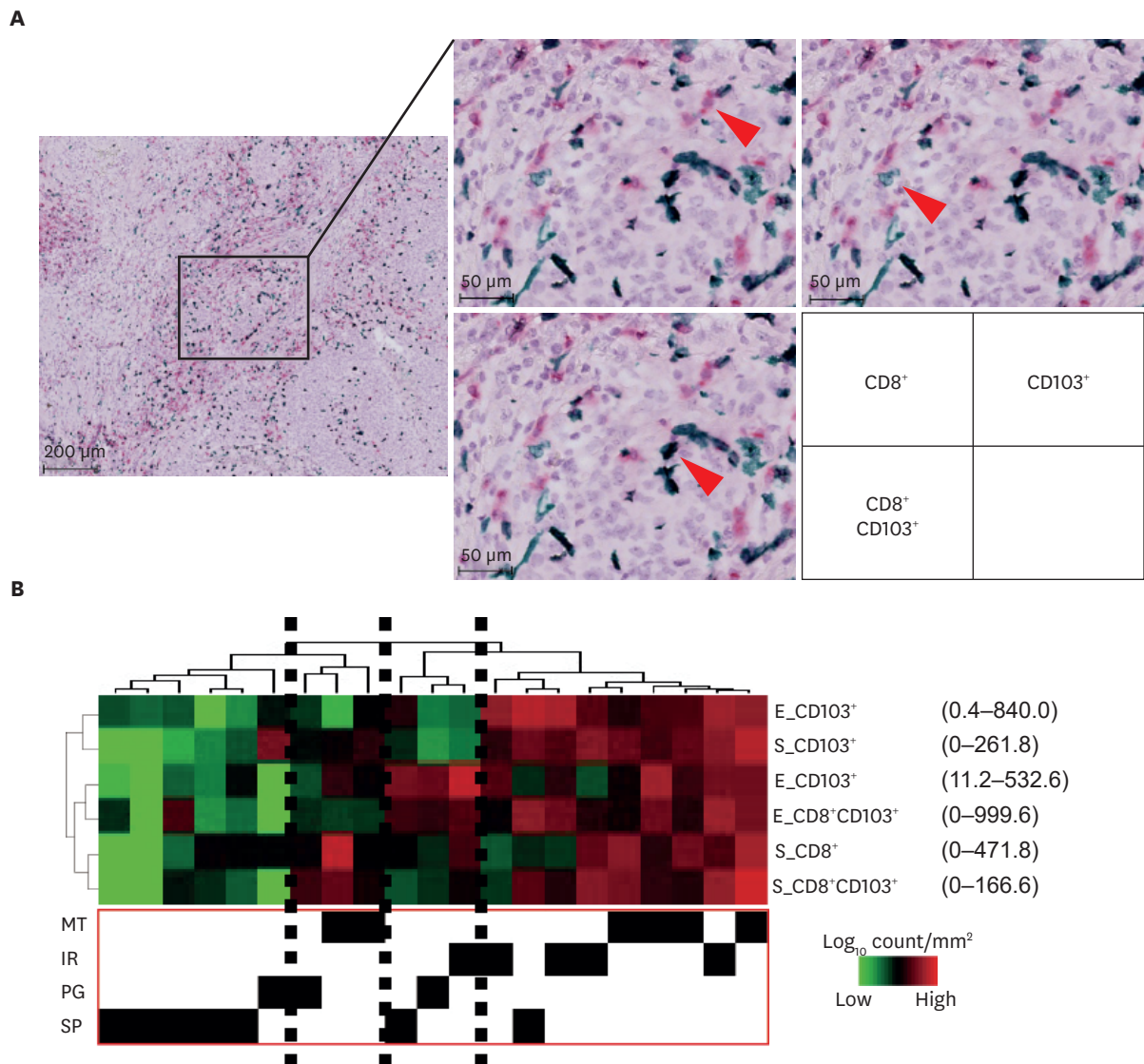
Fig. 4. Association of histopathological subtypes of high-grade serous ovarian cancer and tumor-infiltrating lymphocytes. (A) Representative image of immunohistochemical staining. Arrowhead shows lymphocytes. CD8+ T cells; fast red, CD103+ cells; hist green, double positive cells; black. (B) Hierarchical clustering with tumor-infiltrating lymphocytes.
E, epithelial component, IR, immune reactive; MT, mesenchymal transition; MVD, microvascular density; PG, papilloglandular; S, stromal component; SP, solid and proliferative.

Analysis of tumor immunity

We focused on tissue resident lymphocytes [23] and performed double immunohistochemistry for CD8 and CD103 (**Fig. 4**). We evaluated the number of CD8 positive, CD103 positive, and CD8 and CD103 double positive cells in the epithelium or stroma in 21 recent cases of the Kindai/Kyoto cohort and performed hierarchical clustering. Tumor clusters with high infiltration of immune cells were observed, which contained almost exclusively MT or IR types (**Fig. 4**).

DISCUSSION

When we developed the histopathologic subtyping of HGSOC in our previous study, we selected 5 typical cases for each of the 4 subtypes and used a total of 20 glass slides as a

training set. We then tested for inter-observer agreement in another 28 cases with 6 observers [12]. The main objective of the current study was to modify the histopathological subtyping of HGSOC into a definitive classification using WSI. Making pathological diagnosis by WSI has significant advantages in terms of consultation, information sharing, and application to AI. However, unlike glass slide, WSI is difficult to observe cells in detail, and therefore, certain modifications are required to use WSI for pathological diagnosis [24,25]. In this study, 102 cases in TCGA were used for training by 4 observers. The Kindai/Kyoto cohort (59 cases) was then independently evaluated by the 4 observers (**Table 2**). Thus, a total of 161 cases with WSI were used in this study, and our results proved the reproducibility of this pathological subtyping diagnosis by validating inter-observer agreement rate in a much larger number of cases compared with that in our previous study. Recently, 7 gynecologic pathologists independently reviewed HE specimens of 75 cases of endocervical adenocarcinoma and compared the International Endocervical Adenocarcinoma Criteria and Classification with the World Health Organization classification [26]. They reported that the former was superior in terms of inter-observer agreement, with Kappa coefficients of 0.46 vs. 0.3 and perfect agreement (7/7 matched) in 42 cases (56%) vs. 7 cases (10%), which results are similar to the present study. Therefore, the Kappa coefficients and concordance rates in the present study are considered acceptable as a new histopathological diagnosis.

HGSOC is the most frequent cancer type with HRD because of *BRCA1/2* mutations, *BRCA1* promoter methylation, and alterations in other DNA homologous recombination pathway genes [27]. HRD accounts for approximately half of all HGSOC and leads to platinum and PARP inhibitor sensitivity [3]. Therefore, the ability to determine HRD in pathological slides would be clinically useful. SET features have been defined as morphological features observed in HGSOC with *BRCA* gene mutations. In a previous study, SET features were examined by a single observer, who found SET features in 22/31 cases with *BRCA* alterations and 2/12 cases without *BRCA* alterations in the training set and 9/9 cases with *BRCA1* alterations and 9/14 cases without *BRCA1* alterations in the validation set [15]. In a subsequent report of cases evaluated by 2 observers, SET was found in 13/26 cases with germline *BRCA1/2* mutations and 9/32 cases without germline *BRCA1/2* mutations, with no statistically significant difference in their frequencies [28]. When we examined the WSI data of TCGA, we found no association between SET features and *BRCA* alterations (**Fig. S3**). In previous papers, all HE slides of the tumor were examined, and our observation of WSI of tumor representative images may have been insufficient to evaluate SET features. However, previous reports have had several problems, including small sample size, insufficient consideration of inter-observer variability, and different frequencies of tumors with SET features between training and test sets and between papers. Hence, we have doubts about the reproducibility of the association between SET and *BRCA* alterations. At present, it seems difficult to predict *BRCA* alterations and HRD, at least by observation of WSI.

In this study we focused our analysis specifically on treatment individualization of the MT type. The WSI classification of only a representative part of the tumor may differ from the classification of the whole tumor because of intratumor heterogeneity. However, we previously demonstrated that diagnosis of the MT type is reproducible in the same individual even when the tumor specimen collection sites are different [12]. In this study, we found that the ssGSEA score of HALLMARK_EPITHELIAL_MESENCHYMAL_TRANSITION, which characterizes the mesenchymal gene expression subtype [22], was significantly higher in the MT type (**Fig. 2**), suggesting that the tumor site used for HE specimen preparation has the same characteristics as the site where gene expression analysis was performed.

A group of genes whose expression was downregulated by anti-VEGF antibody (VEGF-dependent genes), including *PECAM1*, which encodes CD31, correlated with sensitivity to the anti-VEGF antibody bevacizumab in colorectal cancer [29]. In HGSOC, overexpression of VEGF-dependent genes was found in the mesenchymal type, which correlated with poor prognosis [30]. In our study, we found that genes related to angiogenesis were upregulated in the MT type, and CD31-positive MVD was high (**Fig. 3**). In the data analysis of the GOG218 study, CD31-positive MVD high was a predictive marker for bevacizumab sensitivity [31], suggesting that bevacizumab may be more effective in the MT type. Furthermore, the mesenchymal type determined by gene expression [32] and the MT type evaluated by histopathology [12] are associated with residual tumor at surgery, and bevacizumab is more effective in patients with more residual tumor at surgery [5]. WSI data from the GOG218 study [4] and the ICON7 study [5], which randomized patients with and without bevacizumab, should be reviewed in future studies to determine whether the effect of bevacizumab is enhanced in the MT type.

It has been reported that the "mesenchymal type" in the TCGA gene expression subtype classification includes cases with a high immune response [33]. In this study, we found an enrichment of gene ontology terms related to immune response in genes that are highly expressed in the histopathological MT type (**Fig. 2**). Recently, CD103 has been used as a marker for tissue resident T cells and natural killer cells [34], and infiltration of CD103-positive resident memory-like CD8$^+$ T cells is expected to be a biomarker for predicting the effect of immune checkpoint inhibitors (ICIs) [35]. In this study, we found CD8$^+$, CD103$^+$, and CD8$^+$CD103$^+$ immune cell infiltration in MT and IR, and almost no infiltration in SP and PG (**Fig. 3**). In a recent phase 3 study for ovarian cancer, the efficacy of ICIs was not proven [36,37], but it may be useful to examine whether ICIs show efficacy in MT and IR.

In the JGOG3016 trial of advanced ovarian cancer, ddTC with an increased dose of paclitaxel prolonged PFS compared with TC, but there was no significant difference in the larger phase 3 trial ICON8 [8]. However, in ICON8, the median PFS was prolonged by approximately 3 months in the ddTC group compared with that in the TC group [8]. Because ddTC was more beneficial than TC in MT patients in our JGOG3016A1 study [13], if the ICON8 cohort is divided into MT and non-MT types by WSI, ddTC may prove to be useful in MT type.

The identification of histopathological subtyping by WSI will lead to the establishment of a classification method by AI or machine learning. Convolutional neural networks have been able to classify the entire TCGA slide image into 19 cancer types and even subtypes [38]. The deep learning system also diagnosed Gleason grading of prostate needle biopsy specimens more accurately than a general pathologist [39]. The histotype diagnosis of ovarian cancer was also predicted with high accuracy by machine learning [40]. The results of this study provide basic information for the development of a machine learning program for histopathological subtyping of HGSOC. Although the interobserver agreement based on human observation was not perfect, the establishment of AI diagnostics will allow for more reproducible histopathological subtyping.

In conclusion, we have modified our previous algorithm to perform histopathological subtyping of HGSOC reproducibly using WSI. In this study, we used publicly available TCGA data as a training set so that pathologists around the world can learn this diagnostic method and apply it to clinical practice immediately. We found that the MT type had increased angiogenesis and high tumor immune activity. If we can evaluate the WSI enrolled in

bevacizumab, ICI or ddTC clinical trials and classify the cases into MT type and non-MT type, and prove the difference in therapeutic effects, the personalized treatment of HGSOC will be advanced. The application of the results of this study to machine learning is expected to further improve the objectivity of diagnosis and advance its application to general practice.

SUPPLEMENTARY MATERIALS

Data S1
New algorithm of histopathological subtyping of high-grade serous ovarian cancer

Click here to view

Data S2
QuPath analysis of CD31 immunohistochemistry

Click here to view

Table S1
Initial inter-observer concordance rates for The Cancer Genome Atlas samples

Click here to view

Table S2
The Cancer Genome Atlas cases

Click here to view

Table S3
Highly expressed genes in the mesenchymal transition type

Click here to view

Table S4
Enriched gene ontology terms in the highly expressed genes in the mesenchymal transition type

Click here to view

Table S5
Clinical characteristics of the Kindai/Kyoto cohort

Click here to view

Table S6
Kindai/Kyoto cohort

Click here to view

Fig. S1
Evaluation of the percentage of lymphocytes infiltrating the tumor stroma.

Click here to view

Fig. S2

Undetermined cases in TCGA samples. (TCGA 23-1118) (TCGA 23-1121) Mostly stromal tissue with no epithelial structure. (TCGA VG-A8LO) This was frozen sections and unsuitable for detailed histological analysis. (TCGA 23-1110) Complex epithelial arrangement with relatively little intervening stroma, not easily identified as cribriform, papillary, or solid. (TCGA 23-1120) Similar to many other types of carcinomas, high grade serous carcinomas can have a more ragged architecture in the tumor invasive front and/or around intratumoral fibrosis. In PG/SP pattern-predominant cases, this can result in PG/SP pattern gradually transitioning to mesenchymal transition pattern in the invasive front or around fibrosis.

Click here to view

Fig. S3

Histopathological subtype and HRD status. (A) Association of *BRCA* alterations and HRD scores with the histopathological subtypes. There was no association between them. (B) Association between histopathological subtypes and SET cases (SET feature ≥50%). (C) Association between SET and *BRCA* alterations. (D) Association between SET and HRD scores.

Click here to view

REFERENCES

1. Siegel RL, Miller KD, Fuchs HE, Jemal A. Cancer statistics, 2021. CA Cancer J Clin 2021;71:7-33.
   PUBMED | **CROSSREF**

2. Seidman JD, Horkayne-Szakaly I, Haiba M, Boice CR, Kurman RJ, Ronnett BM. The histologic type and stage distribution of ovarian carcinomas of surface epithelial origin. Int J Gynecol Pathol 2004;23:41-4.
   PUBMED | **CROSSREF**

3. Nakai H, Matsumura N. Individualization in the first-line treatment of advanced ovarian cancer based on the mechanism of action of molecularly targeted drugs. Int J Clin Oncol 2022;27:1001-12.
   PUBMED | **CROSSREF**

4. Burger RA, Brady MF, Bookman MA, Fleming GF, Monk BJ, Huang H, et al. Incorporation of bevacizumab in the primary treatment of ovarian cancer. N Engl J Med 2011;365:2473-83.
   PUBMED | **CROSSREF**

5. Perren TJ, Swart AM, Pfisterer J, Ledermann JA, Pujade-Lauraine E, Kristensen G, et al. A phase 3 trial of bevacizumab in ovarian cancer. N Engl J Med 2011;365:2484-96.
   PUBMED | **CROSSREF**

6. Katsumata N, Yasuda M, Takahashi F, Isonishi S, Jobo T, Aoki D, et al. Dose-dense paclitaxel once a week in combination with carboplatin every 3 weeks for advanced ovarian cancer: a phase 3, open-label, randomised controlled trial. Lancet 2009;374:1331-8.
   PUBMED | **CROSSREF**

7. Katsumata N, Yasuda M, Isonishi S, Takahashi F, Michimae H, Kimura E, et al. Long-term results of dose-dense paclitaxel and carboplatin versus conventional paclitaxel and carboplatin for treatment of advanced epithelial ovarian, fallopian tube, or primary peritoneal cancer (JGOG 3016): a randomised, controlled, open-label trial. Lancet Oncol 2013;14:1020-6.
   PUBMED | **CROSSREF**

8. Clamp AR, James EC, McNeish IA, Dean A, Kim JW, O'Donnell DM, et al. Weekly dose-dense chemotherapy in first-line epithelial ovarian, fallopian tube, or primary peritoneal carcinoma treatment (ICON8): primary progression free survival analysis results from a GCIG phase 3 randomised controlled trial. Lancet 2019;394:2084-95.
   PUBMED | **CROSSREF**

9. Cancer Genome Atlas Research Network. Integrated genomic analyses of ovarian carcinoma. Nature 2011;474:609-15.
   PUBMED | **CROSSREF**

10. Kommoss S, Winterhoff B, Oberg AL, Konecny GE, Wang C, Riska SM, et al. Bevacizumab may differentially improve ovarian cancer outcome in patients with proliferative and mesenchymal molecular subtypes. Clin Cancer Res 2017;23:3794-801.
    PUBMED | **CROSSREF**

11. Murakami R, Matsumura N, Brown JB, Wang Z, Yamaguchi K, Abiko K, et al. Prediction of taxane and platinum sensitivity in ovarian cancer based on gene expression profiles. Gynecol Oncol 2016;141:49-56.
    PUBMED | **CROSSREF**

12. Murakami R, Matsumura N, Mandai M, Yoshihara K, Tanabe H, Nakai H, et al. Establishment of a novel histopathological classification of high-grade serous ovarian carcinoma correlated with prognostically distinct gene expression subtypes. Am J Pathol 2016;186:1103-13.
    PUBMED | **CROSSREF**

13. Murakami R, Matsumura N, Michimae H, Tanabe H, Yunokawa M, Iwase H, et al. The mesenchymal transition subtype more responsive to dose dense taxane chemotherapy combined with carboplatin than to conventional taxane and carboplatin chemotherapy in high grade serous ovarian carcinoma: a survey of Japanese Gynecologic Oncology Group study (JGOG3016A1). Gynecol Oncol 2019;153:312-9.
    PUBMED | **CROSSREF**

14. Takaya H, Nakai H, Takamatsu S, Mandai M, Matsumura N. Homologous recombination deficiency status-based classification of high-grade serous ovarian carcinoma. Sci Rep 2020;10:2757.
    PUBMED | **CROSSREF**

15. Soslow RA, Han G, Park KJ, Garg K, Olvera N, Spriggs DR, et al. Morphologic patterns associated with BRCA1 and BRCA2 genotype in ovarian carcinoma. Mod Pathol 2012;25:625-36.
    PUBMED | **CROSSREF**

16. Broberg P. Statistical methods for ranking differentially expressed genes. Genome Biol 2003;4:R41.
    PUBMED | **CROSSREF**

17. Pomaznoy M, Ha B, Peters B. GOnet: a tool for interactive Gene Ontology analysis. BMC Bioinformatics 2018;19:470.
    PUBMED | **CROSSREF**

18. Marien KM, Croons V, Waumans Y, Sluydts E, De Schepper S, Andries L, et al. Development and validation of a histological method to measure microvessel density in whole-slide images of cancer tissue. PLoS One 2016;11:e0161496.
    PUBMED | **CROSSREF**

19. Vang R, Levine DA, Soslow RA, Zaloudek C, Shih IM, Kurman RJ. Molecular alterations of tp53 are a defining feature of ovarian high-grade serous carcinoma: a rereview of cases lacking TP53 mutations in The Cancer Genome Atlas ovarian study. Int J Gynecol Pathol 2016;35:48-55.
    PUBMED | **CROSSREF**

20. Salgado R, Denkert C, Demaria S, Sirtaine N, Klauschen F, Pruneri G, et al. The evaluation of tumor-infiltrating lymphocytes (TILs) in breast cancer: recommendations by an International TILs Working Group 2014. Ann Oncol 2015;26:259-71.
    PUBMED | **CROSSREF**

21. Kos Z, Roblin E, Kim RS, Michiels S, Gallas BD, Chen W, et al. Pitfalls in assessing stromal tumor infiltrating lymphocytes (sTILs) in breast cancer. NPJ Breast Cancer 2020;6:17.
    PUBMED | **CROSSREF**

22. Liberzon A, Birger C, Thorvaldsdóttir H, Ghandi M, Mesirov JP, Tamayo P. The Molecular Signatures Database (MSigDB) hallmark gene set collection. Cell Syst 2015;1:417-25.
    PUBMED | **CROSSREF**

23. Anadon CM, Yu X, Hänggi K, Biswas S, Chaurio RA, Martin A, et al. Ovarian cancer immunogenicity is governed by a narrow subset of progenitor tissue-resident memory T cells. Cancer Cell 2022;40:545-557.e13.
    PUBMED | **CROSSREF**

24. Pantanowitz L, Sinard JH, Henricks WH, Fatheree LA, Carter AB, Contis L, et al. Validating whole slide imaging for diagnostic purposes in pathology: guideline from the College of American Pathologists Pathology and Laboratory Quality Center. Arch Pathol Lab Med 2013;137:1710-22.
    PUBMED | **CROSSREF**

25. Evans AJ, Brown RW, Bui MM, Chlipala EA, Lacchetti C, Milner DA, et al. Validating whole slide imaging systems for diagnostic purposes in pathology. Arch Pathol Lab Med 2022;146:440-50.
    PUBMED | **CROSSREF**

26. Hodgson A, Park KJ, Djordjevic B, Howitt BE, Nucci MR, Oliva E, et al. International endocervical adenocarcinoma criteria and classification: validation and interobserver reproducibility. Am J Surg Pathol 2019;43:75-83.
    PUBMED | **CROSSREF**

27. Takamatsu S, Brown JB, Yamaguchi K, Hamanishi J, Yamanoi K, Takaya H, et al. Utility of homologous recombination deficiency biomarkers across cancer types. JCO Precis Oncol 2022;6:e2200085.
PUBMED | CROSSREF

28. Howitt BE, Hanamornroongruang S, Lin DI, Conner JE, Schulte S, Horowitz N, et al. Evidence for a dualistic model of high-grade serous carcinoma: BRCA mutation status, histology, and tubal intraepithelial carcinoma. Am J Surg Pathol 2015;39:287-93.
PUBMED | CROSSREF

29. Brauer MJ, Zhuang G, Schmidt M, Yao J, Wu X, Kaminker JS, et al. Identification and analysis of in vivo VEGF downstream markers link VEGF pathway activity with efficacy of anti-VEGF therapies. Clin Cancer Res 2013;19:3681-92.
PUBMED | CROSSREF

30. Yin X, Wang X, Shen B, Jing Y, Li Q, Cai MC, et al. A VEGF-dependent gene signature enriched in mesenchymal ovarian cancer predicts patient prognosis. Sci Rep 2016;6:31079.
PUBMED | CROSSREF

31. Bais C, Mueller B, Brady MF, Mannel RS, Burger RA, Wei W, et al. Tumor microvessel density as a potential predictive marker for bevacizumab benefit: GOG-0218 biomarker analyses. J Natl Cancer Inst 2017;109:djx066.
PUBMED | CROSSREF

32. Riester M, Wei W, Waldron L, Culhane AC, Trippa L, Oliva E, et al. Risk prediction for late-stage ovarian cancer by meta-analysis of 1525 patient samples. J Natl Cancer Inst 2014;106:dju048.
PUBMED | CROSSREF

33. Verhaak RG, Tamayo P, Yang JY, Hubbard D, Zhang H, Creighton CJ, et al. Prognostically relevant gene signatures of high-grade serous ovarian carcinoma. J Clin Invest 2013;123:517-25.
PUBMED | CROSSREF

34. Dornieden T, Sattler A, Pascual-Reguant A, Ruhm AH, Thiel LG, Bergmann YS, et al. Signatures and specificity of tissue-resident lymphocytes identified in human renal peritumor and tumor tissue. J Am Soc Nephrol 2021;32:2223-41.
PUBMED | CROSSREF

35. Dhodapkar MV, Dhodapkar KM. Tissue-resident memory-like T cells in tumor immunity: clinical implications. Semin Immunol 2020;49:101415.
PUBMED | CROSSREF

36. Monk BJ, Colombo N, Oza AM, Fujiwara K, Birrer MJ, Randall L, et al. Chemotherapy with or without avelumab followed by avelumab maintenance versus chemotherapy alone in patients with previously untreated epithelial ovarian cancer (JAVELIN Ovarian 100): an open-label, randomised, phase 3 trial. Lancet Oncol 2021;22:1275-89.
PUBMED | CROSSREF

37. Moore KN, Bookman M, Sehouli J, Miller A, Anderson C, Scambia G, et al. Atezolizumab, bevacizumab, and chemotherapy for newly diagnosed stage III or IV ovarian cancer: placebo-controlled randomized phase III trial (IMagyn050/GOG 3015/ENGOT-OV39). J Clin Oncol 2021;39:1842-55.
PUBMED | CROSSREF

38. Noorbakhsh J, Farahmand S, Foroughi Pour A, Namburi S, Caruana D, Rimm D, et al. Deep learning-based cross-classifications reveal conserved spatial behaviors within tumor histological images. Nat Commun 2020;11:6367.
PUBMED | CROSSREF

39. Nagpal K, Foote D, Tan F, Liu Y, Chen PC, Steiner DF, et al. Development and validation of a deep learning algorithm for Gleason grading of prostate cancer from biopsy specimens. JAMA Oncol 2020;6:1372-80.
PUBMED | CROSSREF

40. Farahani H, Boschman J, Farnell D, Darbandsari A, Zhang A, Ahmadvand P, et al. Deep learning-based histotype diagnosis of ovarian carcinoma whole-slide pathology images. Mod Pathol 2022;35:1983-90.
PUBMED | CROSSREF